



ISSN: 1813-162X (Print); 2312-7589 (Online)

Tikrit Journal of Engineering Sciences

available online at: <http://www.tj-es.com>
TJES
Tikrit Journal of
Engineering Sciences

Studying Heat-Affected Zone, Surface Roughness and Material Removal Rate in NPMEDM Process for Inconel 718 Using Nano Silicon Carbide Powder

Dunia A. Ghulam *, Abbas F. Ibrahim

Production Engineering and Metallurgy Department, University of Technology, Baghdad, Iraq.

Keywords:

HAZ; Inconel 718; MF; MRR; NPMEDM; SR; Surfactant.

Highlights:

- The performance of the NPMEDM process was improved.
- After powder addition, WLT and SR were decreased, and MRR was increased.
- Nano SiC powder concentration significantly affected responses compared to other parameters.

ARTICLE INFO

Article history:

Received	08 July	2023
Received in revised form	25 July	2023
Accepted	26 Jan.	2024
Final Proofreading	20 Nov.	2024
Available online	20 Mar.	2025

© THIS IS AN OPEN ACCESS ARTICLE UNDER THE CC BY LICENSE. <http://creativecommons.org/licenses/by/4.0/>



Citation: Ghulam DA, Ibrahim AF. Studying Heat-Affected Zone, Surface Roughness and Material Removal Rate in NPMEDM Process for Inconel 718 Using Nano Silicon Carbide Powder. *Tikrit Journal of Engineering Sciences* 2025; 32(1): 1338. <http://doi.org/10.25130/tjes.32.1.11>

*Corresponding author:


Dunia A. Ghulam

Production Engineering and Metallurgy Department,
University of Technology, Baghdad, Iraq.

Abstract: Nano powder mixed electrical discharge machining (NPMEDM) is one of the non-traditional machining processes employed to machine metals, which can be tough to machine using traditional processes. It is accomplished by adding conductive powders to dielectric fluid to enhance the performance of the process. In this paper, several experiments were conducted to enhance the process performance in terms of white layer thickness (WLT), heat affected zone (HAZ), surface roughness (SR), and material removal rate (MRR) of the Inconel 718 alloy, machined using Nano SiC powder added to soybean oil, used as a dielectric fluid. The chosen process variables were discharge current, pulse on time, powder concentration, and magnetic field. Experimental outcomes revealed that adding 2 g/l Nano SiC to soybean oil improved the white layer thickness by about 55.16% compared to 0 g/l and 4 g/l additions, while the thickness of heat affected zone increased. Surface roughness and MRR improved when adding 4 g/l of NanoSiC to the dielectric fluid; the improvements were approximately 5.54% and 53.99%, respectively.

دراسة المنطقة المتأثرة بالحرارة وخشونة السطح ومعدل إزالة المواد في عملية التشغيل Inconel 718 باستخدام الشرارة الكهربائية الممزوجة بالبوابدات النانوية باستخدام مسحوق كربيد السليكون النانوي

دنيا عدنان غلام، عباس فاضل ابراهيم

قسم هندسة الانتاج والمعادن / الجامعة التكنولوجية / بغداد، العراق.

الخلاصة

عملية التشغيل باستخدام الشرارة الكهربائية الممزوجة بالمساحيق النانوية هي احدى عمليات التشغيل اللاتقليدية التي تستخدم لتشغيل المعادن صعبة التشغيل باستخدام العمليات التقليدية. تتم هذه العملية باضافة مساحيق موصلة الى السائل العازل لتحسين اداء العملية. في هذه الدراسة تم اجراء عدد من التجارب العملية لتحسين اداء العملية من حيث سمك الطبقة البيضاء، والمنطقة المتأثرة بالحرارة والخشونة السطحية، ومعدل ازالة المعدن لسبيكة Inconel 718 المشغلة باضافة مسحوق كربيد السليكون النانوي الى زيت الصويا المستخدم كسائل عازل. المتغيرات التي تم اختيارها هي تيار التفريغ والشرارة وتركيز المسحوق والمجال المغناطيسي. النتائج العملية بينت أن اضافة ٢ غم/لتر من مسحوق كربيد السليكون النانوي الى زيت الصويا أدى إلى تحسين سمك الطبقة البيضاء بنسبة 55.16% بالمقارنة باضافته بمقدار ٤ غم/لتر و ٠ غم/لتر بينما زاد سمك المنطقة المتأثرة بالحرارة. الخشونة السطحية ومعدل ازالة المعدن تحسنت عند اضافة المسحوق بتركيز ٤ غم/لتر ونسبة التحسين كانت حوالي 5.54% و 53.99% على التوالي.

الكلمات الدالة: المنطقة المتأثرة بالحرارة، سبيكة الانكونيل ٧١٨، المجال المغناطيسي، معدل ازالة المعدن، التشغيل بالشرارة الكهربائية الممزوجة بالمساحيق النانوية، مادة التقليل من التوتر السطحي، والخشونة السطحية.

1. INTRODUCTION

One of the thermoelectrical processes is electrical discharge machining (EDM). It is used to machine conductive metals when precise dimensions are required. There is no contact between the tool electrode and the machined part; therefore, it does not depend on the mechanical properties of the machined part [1]. In EDM, a plasma channel is formed between the machined workpiece and the tool. EDM can be used to machine electrically conductive super alloys like Inconel, used in different applications, such as electrical power plant equipment, nuclear reactors, the petrochemical industry, and chemical vessels due to its good carburization at elevated temperatures, corrosion resistance, and moderate strength. In the EDM, process dielectric is used as an insulating fluid in which the electrode and the machined workpiece are immersed. Powder mixed electrical discharge machining (PMEDM) is one type of the EDM processes in which the dielectric is mixed with different types of powders to reduce the problem of arcing, increase conductive strength, and increase spark gap distance, enhancing the EDM performance by increasing the material removal rate and surface finish [2]. Researchers have conducted many practical experiments to machine Inconel alloy using various techniques to optimize the machining parameters of the NanoPMEDM process to improve its performance. Basha Shaik Khadar et al. studied the effect of boron carbide powder addition in the insulating fluid to machine Inconel X-750 alloy. The results showed that mixing boron carbide with the insulating fluid resulted in a higher material removal rate, a better surface finish, and a lower recast layer thickness [3]. Thrinadh Jadam et al. reported the machining process of Inconel 718 using PMEDM by adding Multi-Walled Carbon Nanotubes (MWCNTs) to the dielectric. The results showed that adding powder to the

dielectric improved the efficiency of material removal, surface integrity, and tool wear rate of the machined Inconel alloy compared to the conventional EDM process [4]. Karunakaran and Chandrasekaran [5], NPMEDM experiments were conducted on the machine Inconel 800. Different powders were used in this study like, nanotube powders, aluminum, and silicon. When using MWCNT powder, it gave better results than using other powders, reducing the tool wear rate from 22% to 50%, the surface roughness from 29.62% to 41.64%, and enhancing the material removal rate from 42.91% to 53.51% compared to conventional machining. Patel et al. [6] was concluded that discharge current, pulse on time, and aluminum powder concentration were the most significant parameters that affected the surface finish and material removal rate when machining Inconel 718. Amit Kumar et al. observed that the machined surface of Inconel 825 by adding Al_2O_3 Nanopowder in the dielectric was improved, where the microcracks were reduced compared to conventional EDM when using optimal parameters of current, pulse on time, and gap voltage as significant effective parameters [7]. Inconel 718 was machined using graphene nanofluid in [8]. Gap voltage, current, and pulse on time were significant parameters, as the study revealed enhancements in MRR, surface roughness, and TWR of 20.1%, 14%, and 2%, respectively. In the EDM process, debris flushing from the machining gap is one of the challenges. Debris accumulation in the space gap of machining between the machined part and the tool causes short circuits, open circuits, and arcing, inactive pulses. Many researchers have used magnetic fields to improve the EDM process's performance. They concluded that the process of removing debris from the machining gap and EDM performance were improved when using a magnetic field. Preetkanwal Singh Bains et al.

studied the PMEDM process with magnetic field assistance, and the results revealed that the values of microhardness and recast layer thickness were reduced and that higher spark energy, coupled with using a magnetic field, improved MRR and surface finish [9]. Baseri and Sadeghian [10] was concluded that the debris was removed more easily from the machining gap when using a magnetic field, and the MRR, surface roughness, and tool wear rate also improved. The effect of agglomeration, which leads to inhomogeneity in the distribution of powder in the dielectric, is one of the challenges in the PMEDM process; therefore, using surfactants is required. Surfactants are chemicals whose uniform energy distribution can be obtained using them, resulting in a well-defined distribution of powder particles. Powder Mixed Wire Electric Discharge Machining (PMWEDM) to machine Inconel 718 was studied in [11]. A positive effect was obtained on MRR, which improved by 13.56%, and the surface roughness improved by 45.05% when adding powders and surfactant (span 20) to the dielectric. As reported Reddy and Madar [12], surfactant additions to the dielectric increase the dielectric conductivity, and more uniform powder distribution can be obtained, increasing MRR and surface finish. Kolli and Kumar [13], the effect of current, powder (graphite), and surfactant (span 20) concentrations in the dielectric fluid was studied. The results showed that the MRR increased, surface roughness increased, recast layer thickness decreased, and tool wear rate decreased. It was noticed from the literature survey that powder addition to the dielectric improved the EDM process performance, and it is a great scope to study Nanopowder mixed electrical discharge machining with magnetic field assistance, which can be evaluated using different powders to machine different superalloys. Based on the limited studies of machine superalloys like Inconel 718, which

have wide applications, using Nanopowder mixed EDM with magnetic field assists (MF-NPMEDM) process. In this study, Inconel 718 was machined by adding NanoSiC, which was chosen due to its good properties, to biodegradable soybean oil to determine its influence with the magnetic field, peak current, and pulse on time on white layer thickness, surface roughness, and material removal rate.

2. EXPERIMENTAL PROGRAM

2.1. Apparatus and Procedures

The present study used an electrical discharge machine of model CM 323+50N (CHMER EDM) to implement practical experiments. Inconel 718 alloy was used as a workpiece. The specimens' dimensions were (25×10×4) mm. The properties of the workpiece are listed in Table 1. Pure copper with dimensions of (15×10×70) mm was selected as an electrode due to its high electrical and thermal conductivity, excellent corrosion, and wear resistance. The copper properties are listed in Table 2. Nanopowder of SiC (80) nm particles mixed with soybean oil was used as a dielectric for the machining medium. Tween 60 was used as a surfactant; it helps keep the powder particles suspended in the dielectric and not settle to the bottom of the machining tank. Two pieces of permanent magnet (neodymium magnet NdFeB) generate a magnetic field with an intensity of (0.2) T (digital gaussmeter model: DGM-102 was used to measure the magnetic field intensity). Galvanized iron was used to fabricate the machining tank with dimensions of (500×200×250) mm. The tank was provided with a special circulating system consisting of a pump, flushing nozzle, and pipe of 5 mm diameter fixed around the tank's inner walls. Holes with a diameter of 1 mm were made along the length of the pipe to continuously recirculate the dielectric and prevent the powders from settling down in the base of the tank, as shown in Fig. 1.

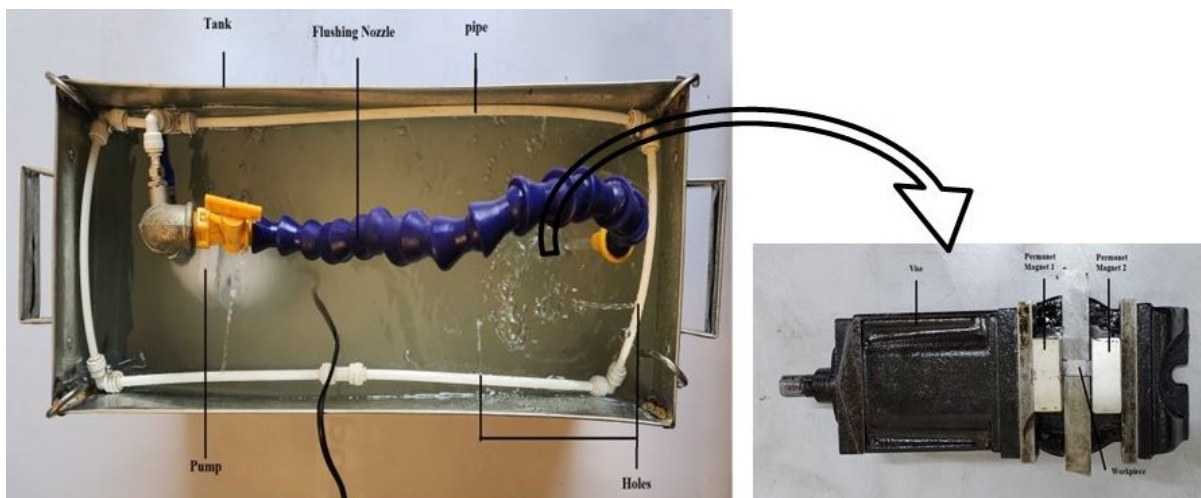


Fig. 1 Machining Tank.

Table 1 Properties of Inconel 718 Supper Alloy.

Properties	Value
Density	8.912 g/cc
Melting point	1260–1335 °C
Ultimate tensile strength	800–1360 MPa
Modulus of elasticity	200 GPa
Thermal conductivity	11.2 W/m.K

Table 2 Properties of Copper Electrode.

Properties	Value
Density	8.96 g/cc
Melting point	1083.4 °C
Thermal conductivity	398 W/(m.K)

2.2. Experimental Procedure

A Multi-level general full factorial design was used to design the experiments and analyze the responses after conducting them. MRR, SR, WLT, and HAZ response features were computed. Table 3 represents the varied parameters and their levels. Apart from these parameters, some were maintained fixed during the machining process; those are listed in Table 4. A snapshot of the specimen machined using these parameters; is shown in Fig. 2.

**Fig. 2** Specimen Before and After Machining.**Table 3** Levels of Variable Parameters.

Parameter	Level 1	Level 2	Level 3
Current (A)	8	16	/
Pulse on time (μs)	100	200	/
Concentration (g/l)	0	2	4
MF (T)	0	0.2	/

Table 4 Used Fixed Parameters.

Parameter	Value
Pulse off time (μs)	75
Powder	SiC
Particle size (nm)	80
Polarity	Straight
Gap voltage (V)	240
Magnetic field intensity (T)	0.2
Surfactant type	Tween 60
Surfactant concentration (ml/l)	1
Depth of cut (mm)	1

3. RESULTS AND DISCUSSION

3.1. Study on Heat-Affected Zone

Many metallurgical changes occurred in the EDMed surface. The affected region is named the heat-affected zone, consisting of some layers, such as the recast layer (white layer) and the hardened layer, located directly below the white layer. When adding SiC, the white thickness layer was reduced compared to the

conventional EDM. When debris was re-solidified, the recast layer formed due to the discharge size during the pulse-off time. The discharging energy increased with the current; therefore, the white layer thickness increased. The temperature in the machining zone was elevated to a high level, leading to higher material removal from the machining zone. The recast layer's thickness increased due to the sedimentation of the debris melted due to insufficient flushing by a dielectric. The white layer thickness decreased after adding SiC because SiC powder particles in the machining gap increased the distance between the electrode and the workpiece, and the plasma channel became wider, decreasing the energy density, according to PMEDM theory [14]. The flushing method efficiency improved due to the enlarged gap distance between the electrode and the machined workpiece using SiC and also due to using a special circulation system. In PMEDM, a wider distance was covered uniformly when discharging, leading to the outspread of the debris uniformly and producing a thinner white layer. At a concentration of (2 g/l) of NanoSiC, a thinner white layer was produced compared to (4 g/l) due to an unstable EDM process that led to short circuits or arcing, producing precipitated material when the concentration of SiC increased to (4 g/l). The experiments were designed using a general full factorial multi-level design by Minitab software 2022. Four input parameters were used, as mentioned in Table 3. The results of the implemented experiments for white layer thickness and hardened layer are shown in Table 5. When the current increased, the white and the hardened layers' thickness also increased. A lower white layer thickness was obtained using a current of (8 A) compared with (16 A) for different concentrations. Also, the increase in pulse on time increased the white layer thickness. The magnetic field effect was small and caused a little increase in the white layer thickness. The effect of SiC concentration and peak current on the thickness of the white layer is shown in Fig. 3. The microscopic pictures for the machined specimens are shown in Fig. 4.

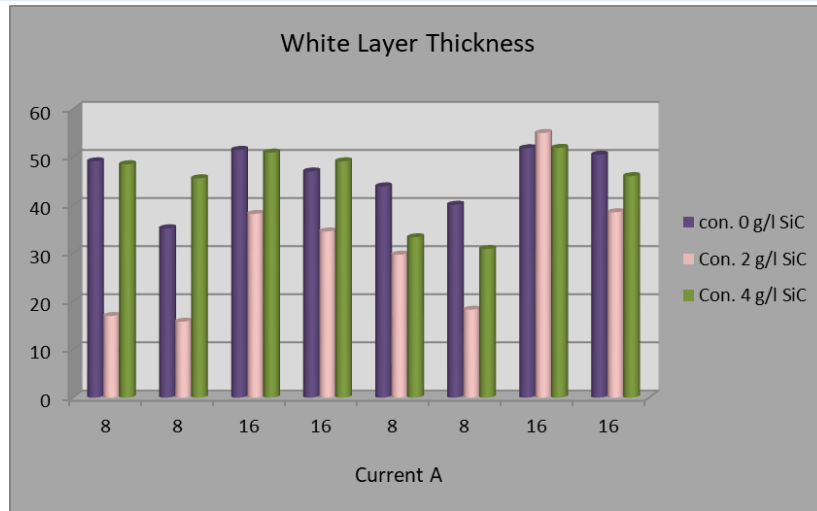
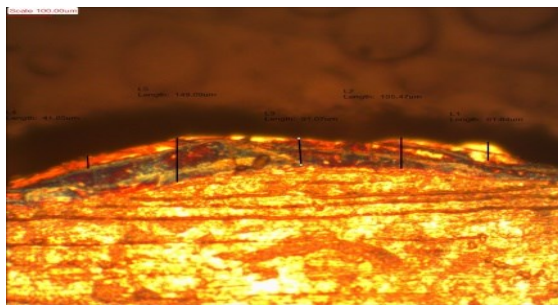


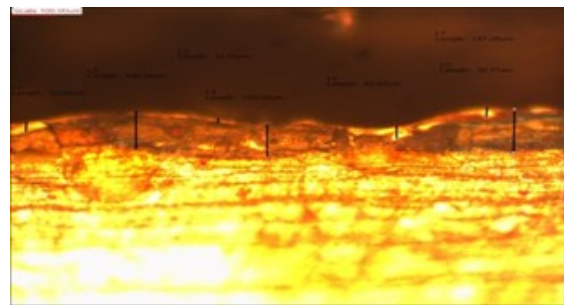
Fig. 3 The Effect of Powder Concentration and Current on WLT.

Table 5 Average WLT and HAZ According to DOE with Optical Microscope Pictures.

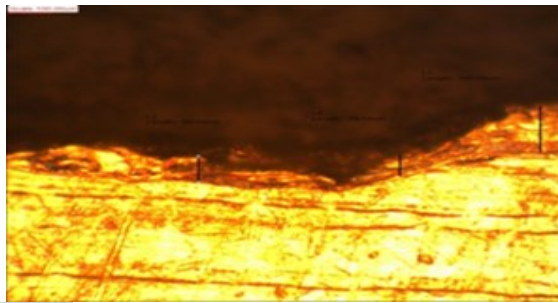
Run	I (A)	Ton (μs)	Con (g/l)	MF (T)	Average WLT (μm)	Average HAZ (μm)	Optical Microscope Picture (Fig.4)
1	16	200	0	0.2	51.845	115.21	Pic. 1
2	8	200	2	0.2	29.71	128.4866667	Pic. 2
3	16	100	4	0.2	46.05	107.8766667	Pic. 3
4	8	100	4	0	45.6	109.7166667	Pic. 4
5	8	200	4	0	48.52	115.71	Pic. 5
6	8	200	0	0	49.12	93.34	Pic. 6
7	8	100	0	0	35.2	94.55	Pic. 7
8	16	100	0	0.2	50.5	73.33	Pic. 8
9	16	100	2	0.2	38.54	155.45	Pic. 9
10	8	100	4	0.2	30.905	163.635	Pic. 10
11	8	200	0	0.2	43.925	137.495	Pic. 11
12	16	200	4	0	50.94	192.73	Pic. 12
13	8	200	2	0	16.96666667	159.3833333	Pic. 13
14	8	100	2	0	15.78333333	156.9666667	Pic. 14
15	16	200	0	0	51.51	111.815	Pic. 15
16	16	200	2	0.2	55.015	232.38	Pic. 16
17	16	100	2	0	34.54	198.71	Pic. 17
18	8	200	4	0.2	33.33	87.87333333	Pic. 18
19	8	100	0	0.2	40.1	92.49	Pic. 19
20	16	200	4	0.2	51.93	190.91	Pic. 20
21	16	200	2	0	38.195	199.09	Pic. 21
22	8	100	2	0.2	18.27	69.085	Pic. 22
23	16	100	4	0	49.12	132.12	Pic. 23
24	16	100	0	0	47.01666667	103.0233333	Pic. 24



Pic. 1 I (16A) Pon (200 μs) Con. (0g) MF (0.2T).



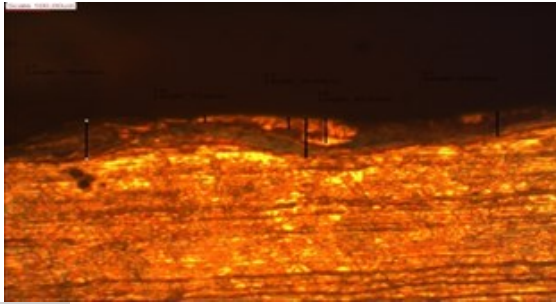
Pic. 2 I (8A) Pon (200 μs) Con. (2g) MF (0.2T).



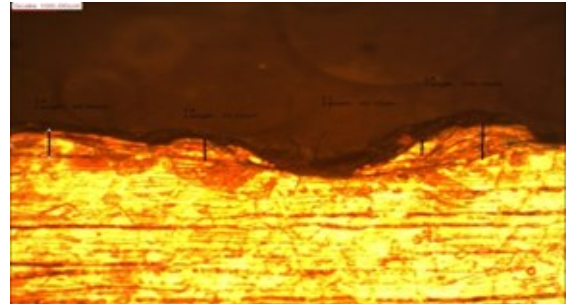
Pic. 3 I (16A) Pon (100 μs) Con. (4g) MF (0.2T).



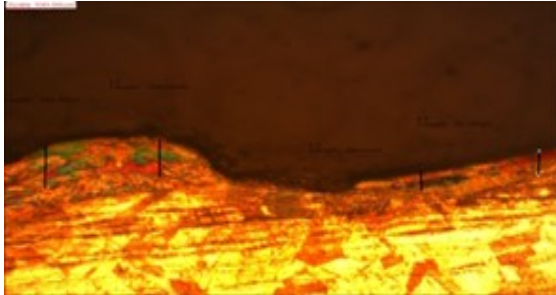
Pic. 4 I (8A) Pon (100 μs) Con. (4g) MF (0 T).



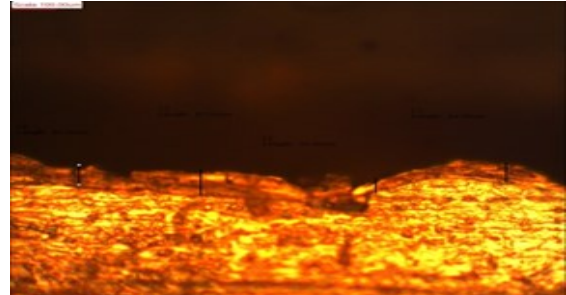
Pic. 5 I (8A) Pon (200 μ s) Con. (4g) MF (0 T).



Pic. 6 I (8A) Pon (200 μ s) Con. (0 g) MF (0 T).



Pic. 7 I (8A) Pon (100 μ s) Con. (0 g) MF (0 T).



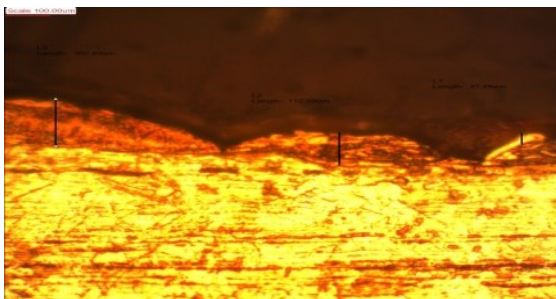
Pic. 8 I (16A) Pon (100 μ s) Con. (0 g) MF (0.2 T).



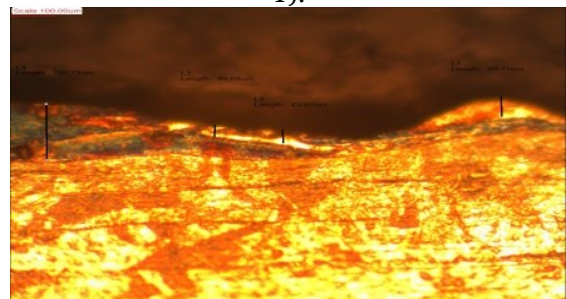
Pic. 9 I (16A) Pon (100 μ s) Con. (2 g) MF (0.2 T).



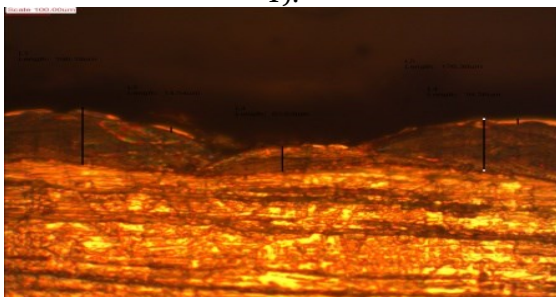
Pic. 10 I (8 A) Pon (100 μ s) Con. (4 g) MF (0.2 T).



Pic. 11 I (8 A) Pon (200 μ s) Con. (0 g) MF (0.2 T).



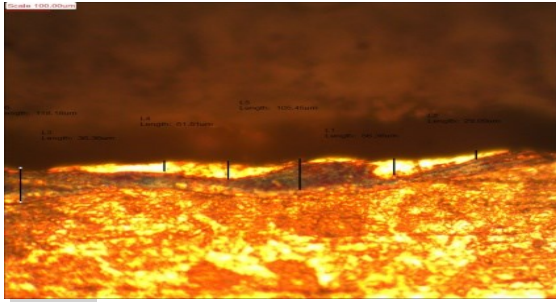
Pic. 12 I (16 A) Pon (200 μ s) Con. (4 g) MF (0 T).



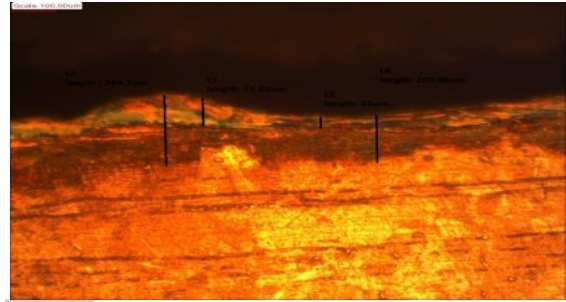
Pic. 13 I (8 A) Pon (200 μ s) Con. (2 g) MF (0 T).



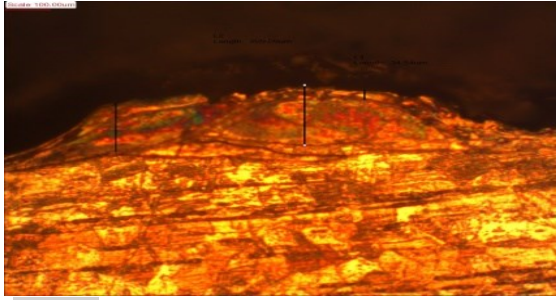
Pic. 14 I (8 A) Pon (100 μ s) Con. (2 g) MF (0 T).



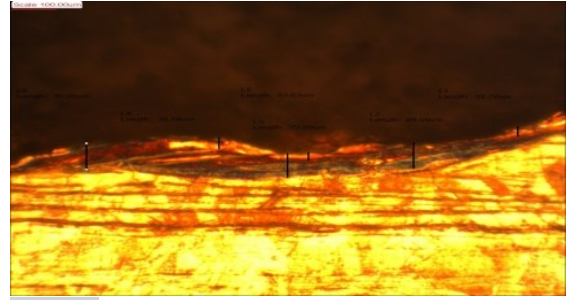
Pic. 15 I (16 A) Pon (200 μ s) Con. (0 g) MF (0 T).



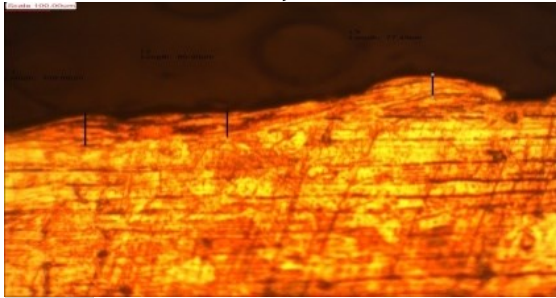
Pic. 16 I (16 A) Pon (200 μ s) Con. (2 g) MF (0.2 T).



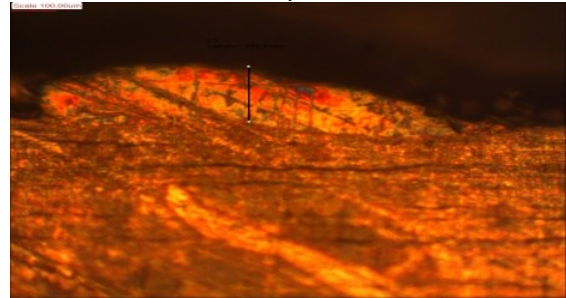
Pic. 17 I (16 A) Pon (100 μ s) Con. (2 g) MF (0 T).



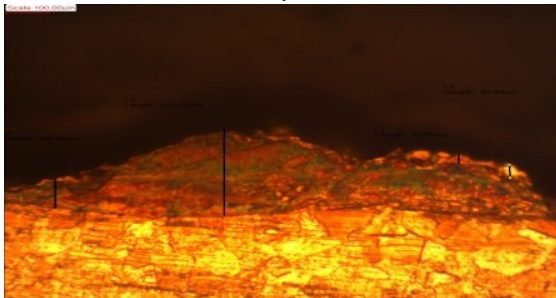
Pic. 18 I (8 A) Pon (200 μ s) Con. (4 g) MF (0.2 T).



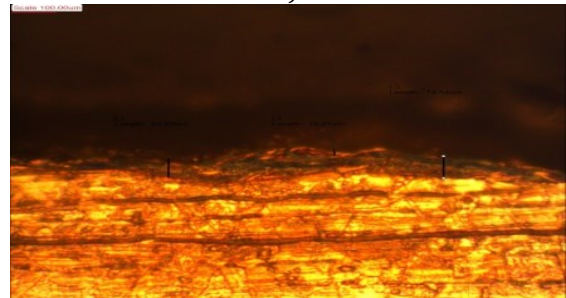
Pic. 19 I (8 A) Pon (100 μ s) Con. (0 g) MF (0.2 T).



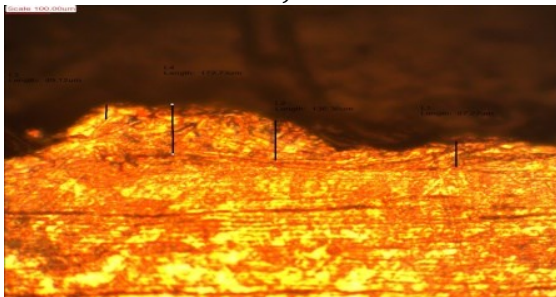
Pic. 20 I (16 A) Pon (200 μ s) Con. (4 g) MF (0.2 T).



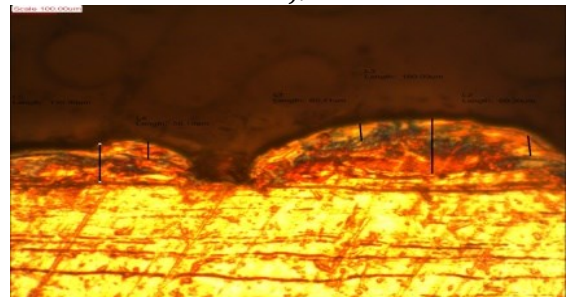
Pic. 21 I (16 A) Pon (200 μ s) Con. (2 g) MF (0 T).



Pic. 22 I (8 A) Pon (100 μ s) Con. (2 g) MF (0.2 T).



Pic. 23 I (16 A) Pon (100 μ s) Con. (4 g) MF (0 T).



Pic. 24 I (16 A) Pon (100 μ s) Con. (0 g) MF (0 T).

Fig. 4 Optical Microscopic Pictures.

According to Table 6, which represents the analysis of variance, the P-value was less than 0.5, i.e., the model was statistically significant. The most effective parameter on WLT was concentration, with 17.63%, followed by current, with 11.2 %, and the effect of pulse on time was 6.27%. The Normal plot for white layer thickness shows that the residuals generally fall on a straight line or very close to

the straight line, meaning errors are distributed normally, as shown in Fig. 5. According to the analysis of variance (see Table 7) for the heat-affected zone, the concentration effect was 8.83%, the effect of current was 8.32%, and the effect of pulse on time was 4.82%. The P-value was less than 0.5, i.e., the model was statistically significant. Figure 6 represents the normal plot.

Table 6 Analysis of Variance for White Layer Thickness.

Source	DF	Adj SS	Adj MS	F-Value	P-Value
Model	6	2572.2	428.70	13.40	0.000
Linear	4	1686.2	421.56	13.18	0.000
I	1	358.2	358.20	11.20	0.004
T on	1	200.6	200.58	6.27	0.023
Con.	2	1127.5	563.74	17.63	0.000
2-Way Interactions	2	886.0	442.99	13.85	0.000
I*Con.	2	886.0	442.99	13.85	0.000
Error	17	543.7	31.98		
Total	23	3115.9			

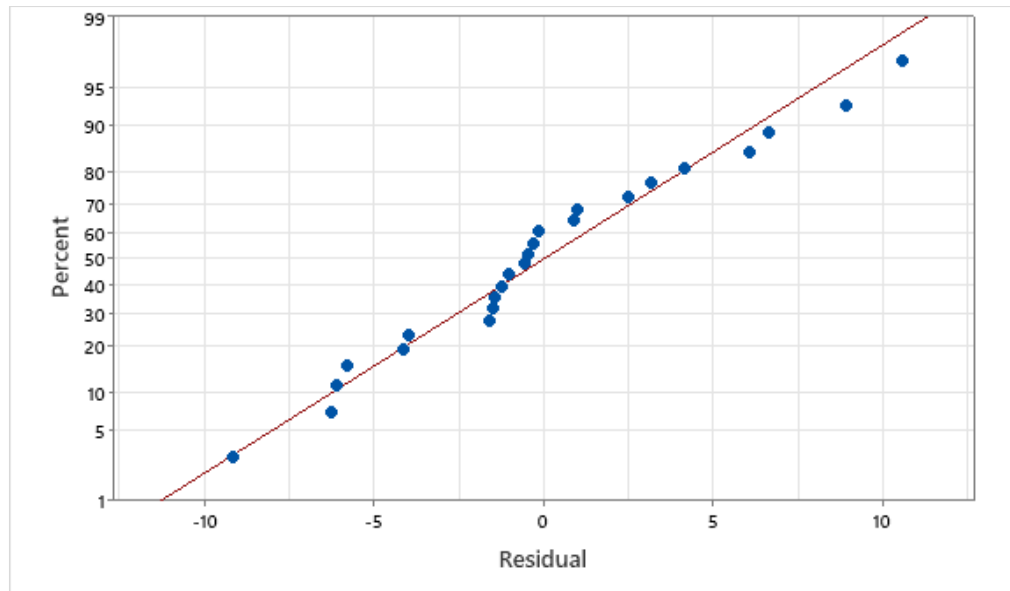


Fig. 5 Normal Plot of White Layer Thickness Analysis.

Table 7 Analysis of Variance for HAZ.

Source	DF	Adj SS	Adj MS	F-Value	P-Value
Model	7	32633	4661.8	5.70	0.002
Linear	4	25169	6292.3	7.70	0.001
I	1	6798	6797.7	8.32	0.011
Ton	1	3939	3939.1	4.82	0.043
Con.	2	14433	7216.3	8.83	0.003
2-Way Interactions	3	7463	2487.7	3.04	0.059
I*Ton	1	2316	2316.3	2.83	0.112
I*Con.	2	5147	2573.4	3.15	0.070
Error	16	13080	817.5		
Total	23	45712			

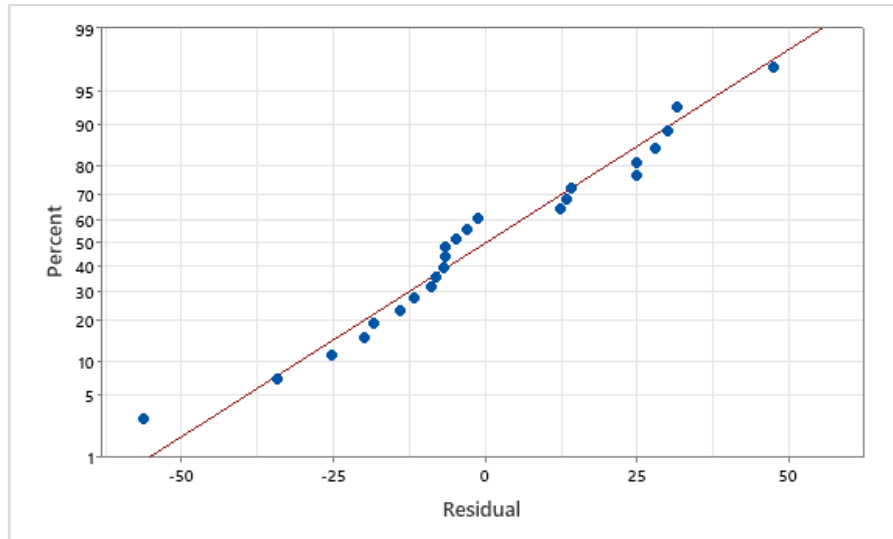


Fig. 6 Normal Plot of HAZ.

3.2. Study on Surface Roughness

SiC has appropriate density and electrical resistivity with high thermal conductivity. In NPMEDM, the Nanoparticles are charged and added to the plasma channel, decreasing the dielectric insulating strength. The gap distance was increased by the servo system controller of the machine. To make the discharge condition stable, in NPMEDM, lower surface roughness was produced because when the plasma channel becomes larger and wider due to the powder addition, the discharge density becomes less on the machining zone, lowering surface roughness and shallower craters [15]. The results of this study achieved lower values of SR compared to the results of [16], in which the values of SR altered from $3.8 \mu\text{m}$ to $8.7 \mu\text{m}$ when the current increased from 3 A to 9 A without powder addition. While adding SiC in the present study reduced the SR values, they

varied from $4.52 \mu\text{m}$ to $5.90 \mu\text{m}$ when the current increased from 8 A to 16 A. The experiment results showed that better surface roughness was obtained for the machined surface at a concentration of 4% of SiC addition in dielectric fluid compared to 2% concentration, i.e., an increase in SiC concentration decreased surface roughness, as shown in Table 8. Increasing current and pulse on time values increased surface roughness. The presence of a magnetic field decreased surface roughness, as clear in the bar chart in Fig. 7. The analysis of variance results in Table 9 showed that the effect of concentration was 38.58%, the most significant factor, followed by the pulse-on-time effect, which was 13%. The magnetic field effect was 4.85%, and the effect of current was 4.80% on surface roughness. The normal plot is shown in Fig. 8.

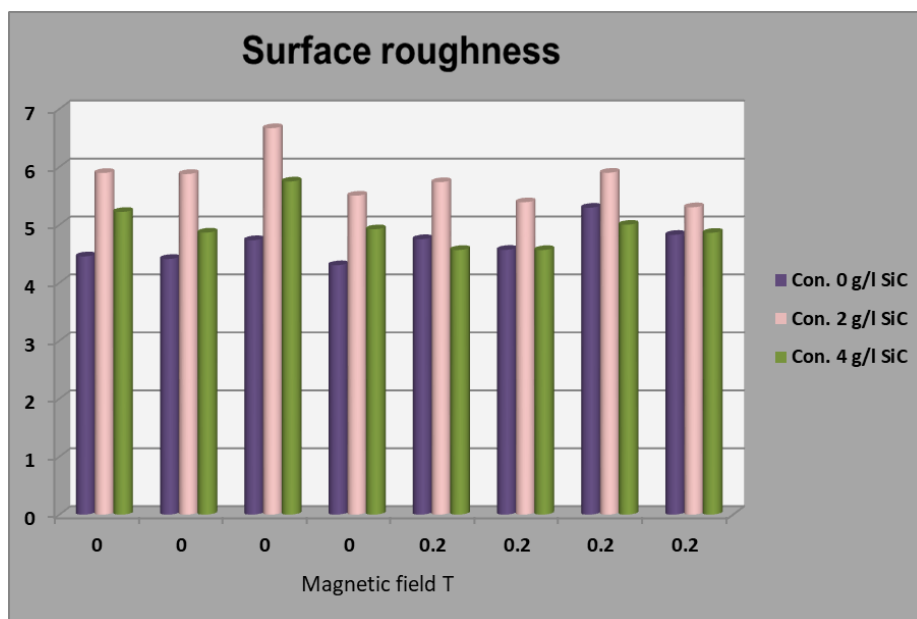


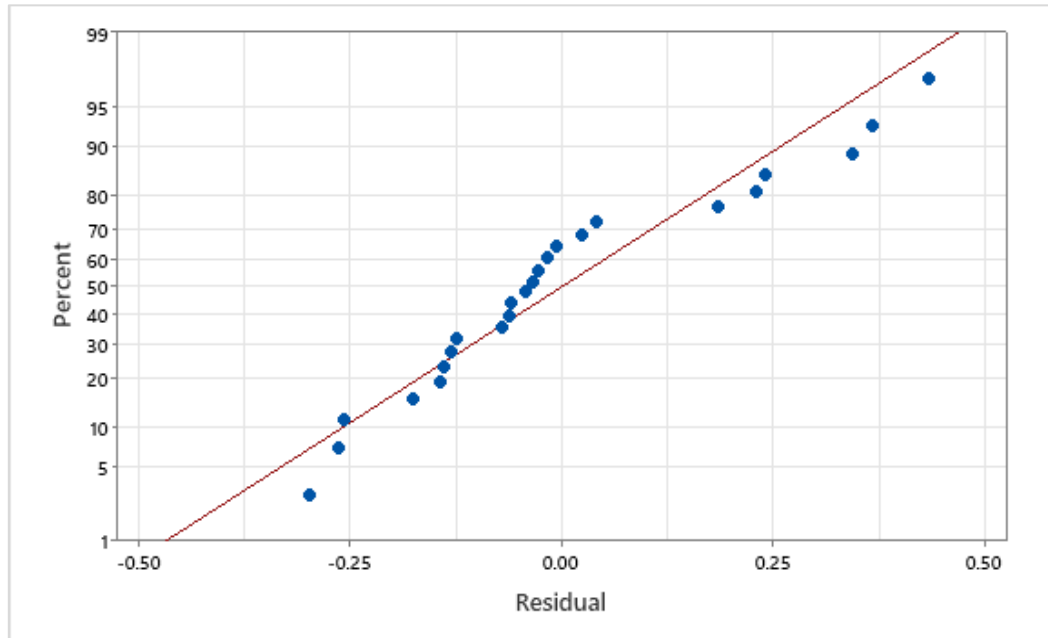
Fig. 7 Effect of Concentration and Magnetic Field of Surface Roughness.

Table 8 Average Surface Roughness for Machined Specimens.

Run	I (A)	Ton (μ s)	Con. (g/l)	MF (T)	Average SR (μ m)
1	16	200	0	0.2	5.296666667
2	8	200	2	0.2	5.737666667
3	16	100	4	0.2	4.863
4	8	100	4	0	4.867333333
5	8	200	4	0	5.223666667
6	8	200	0	0	4.456666667
7	8	100	0	0	4.879333333
8	16	100	0	0.2	4.828
9	16	100	2	0.2	5.304333333
10	8	100	4	0.2	4.560333333
11	8	200	0	0.2	4.753666667
12	16	200	4	0	6.082333333
13	8	200	2	0	5.896333333
14	8	100	2	0	5.878333333
15	16	200	0	0	4.736666667
16	16	200	2	0.2	5.900333333
17	16	100	2	0	5.504333333
18	8	200	4	0.2	4.524333333
19	8	100	0	0.2	4.569333333
20	16	200	4	0.2	5.003
21	16	200	2	0	6.669666667
22	8	100	2	0.2	5.390666667
23	16	100	4	0	4.924333333
24	16	100	0	0	4.304333333

Table 9 Analysis of Variance for Surface Roughness.

Source	DF	Adj SS	Adj MS	F-Value	P-Value
Model	8	7.4736	0.93420	15.00	0.000
Linear	5	6.2154	1.24309	19.96	0.000
I	1	0.2991	0.29912	4.80	0.045
Ton	1	0.8094	0.80936	13.00	0.003
Con.	2	4.8050	2.40250	38.58	0.000
MF	1	0.3020	0.30195	4.85	0.044
2-Way Interactions	3	1.2581	0.41938	6.73	0.004
I*Ton	1	0.5143	0.51431	8.26	0.012
Con.*MF	2	0.7438	0.37192	5.97	0.012
Error	15	0.9342	0.06228		
Total	23	8.4078			

**Fig. 8** Normal Plot for Surface Roughness.

3.3. Study on Material Removal Rate

One of the most essential technological measures in a product's fabrication is MRR; a higher MRR means higher process productivity [17]. Increasing the powder concentration value positively affected the material removal rate

due to the properties of the added NanoSiC particles in soybean oil, producing better MRR than conventional EDM when the results of this study are compared to [18], in which soybean oil was used as a dielectric fluid to machine Inconel 718 alloy without adding powder. After

comparison, it was found that by adding NanoSiC in this study, higher values of MRR were achieved. However, it was found that when the SiC concentration was (4 g/l), better MRR was obtained than (2 g/l), and without adding it into dielectric fluid, also using a magnetic field and increasing the current and pulse on time MRR was increased, as shown in

Fig. 9. Table 10 shows the experimental results of the machined specimens. The analysis of variance for MRR results is shown in Table 11. It is noticed that the current significantly affected MRR (461.08 %). The pulse-on-time effect was (6.36 %), and the concentration effect was (4.96%). Figure 10 represents the normal plot for MRR.

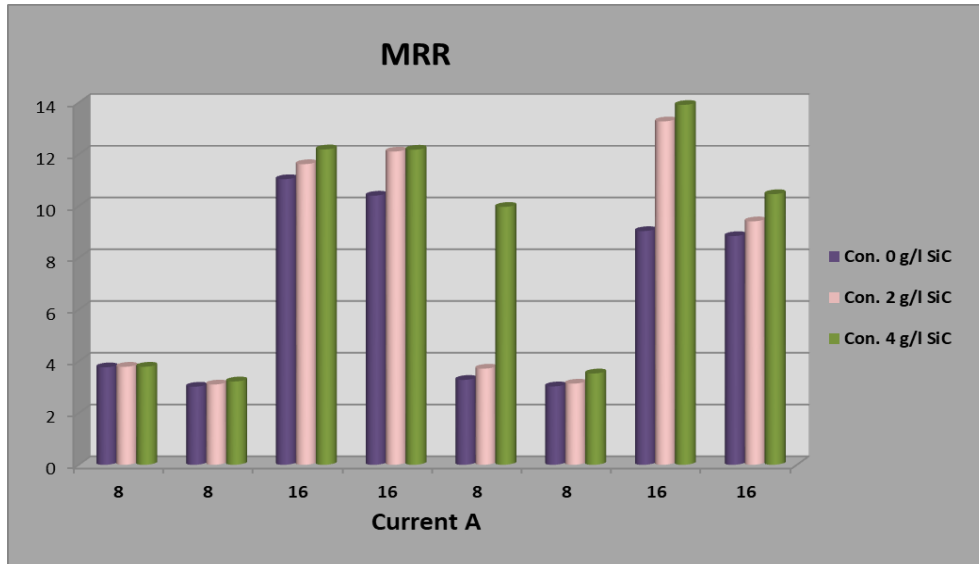


Fig. 9 Effect of Concentration and Current on MRR.

Table 10 Experimental Results for MRR.

Run	I (A)	Ton(μs)	Con.(g/l)	MF(T)	MRR (mm³/min)
1	16	200	0	0.2	9.0325214
2	8	200	2	0.2	3.7159302
3	16	100	4	0.2	10.458378
4	8	100	4	0	3.2212831
5	8	200	4	0	3.7910938
6	8	200	0	0	3.7658696
7	8	100	0	0	3.0183694
8	16	100	0	0.2	8.8388003
9	16	100	2	0.2	9.4099247
10	8	100	4	0.2	3.5304136
11	8	200	0	0.2	3.2820783
12	16	200	4	0	12.187712
13	8	200	2	0	3.7873655
14	8	100	2	0	3.1043354
15	16	200	0	0	11.039118
16	16	200	2	0.2	13.272489
17	16	100	2	0	12.107519
18	8	200	4	0.2	3.9684445
19	8	100	0	0.2	3.030303
20	16	200	4	0.2	13.909591
21	16	200	2	0	11.619111
22	8	100	2	0.2	3.1376528
23	16	100	4	0	12.17809
24	16	100	0	0	10.40126

Table 11 Analysis of Variance for MRR.

Source	DF	Adj SS	Adj MS	F-Value	P-Value
Model	6	378.440	63.073	80.52	0.000
Linear	4	373.934	93.484	119.34	0.000
I	1	361.161	361.161	461.06	0.000
Ton	1	4.982	4.982	6.36	0.022
Con.	2	7.791	3.896	4.97	0.020
2-Way Interactions	2	4.506	2.253	2.88	0.084
I*Con.	2	4.506	2.253	2.88	0.084
Error	17	13.317	0.783		
Total	23	391.757			

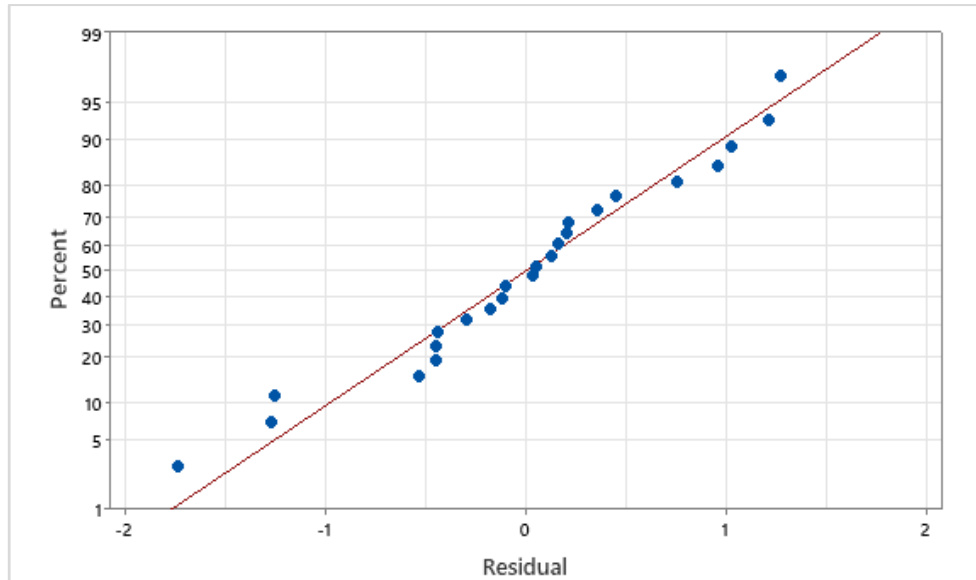


Fig. 10 Normal Plot for MRR.

The present study concluded that using SiC Nanopowders with different concentrations positively reduced the heat-affected zone thickness and improved the surface roughness and machined Inconel 781 specimens' MRR.

4.CONCLUSIONS

The following points could be utilized to summarize the conclusions of the present study:

- Using NanoSiC added to the dielectric during the Inconel 718 machining, the white layer thickness and hardened layer were enhanced compared to the NanoSiC absence. However, a thinner white layer thickness was obtained using NanoSiC powder at a concentration of 2 g/l compared to 4 g/l. The minimum value for white layer thickness was at (2 g/l) of SiC, current (8 A), pulse on time (100 μ s), and magnetic field of (0.2 T). The improvement in WLT was approximately (55.16%).
- Lower surface roughness was obtained for the machined surface at a concentration of (4) g/l compared to a concentration of (2) g/l. Maximum improvement in surface roughness, i.e., 5.54 %, was obtained when (4 g/l) of Nano SiC was used, (16 A) of current, (200 μ s) of pulse on time, and (0.2 T) of magnetic field.
- The material removal rate improved at a concentration of (4 g/l). The maximum improvement for material removal rate, i.e., ~ 53.99%, was at a current of (8 A), a pulse on time of (200 μ s), and (0.2 T).

NOMENCLATURE

NP MEDM	Nanopowder mixed electrical discharge machining.
SiC	Silicon carbide.
SR	Surface roughness μ m
MRR	Material removal rate mm ³ /min
MF	Magnetic field Tesla
I	Current, A
WLT	White layer thickness μ m

HAZ	Heat affected zone μ m
Ton	Pulse on time μ s
Con.	Concentration g/l

REFERENCES

- [1] Abbas AM, Khleif AA. **The Influence of Angled Electrodes on Various Characteristics in EDM Process-Review Article.** *Tikrit Journal of Engineering Sciences* 2023; **30**(2):1–9.
- [2] Dharmendra BV, Kodali SP, Nageswara Rao B. **A Simple and Reliable Taguchi Approach for Multi-Objective Optimization to Identify Optimal Process Parameters in Nano-Powder-Mixed Electrical Discharge Machining of INCONEL800 with Copper Electrode.** *Heliyon* 2019; **5**(8): e02326, (1-9).
- [3] Basha S, Raju M, Kolli M. **Multi-Objective Optimization of Process Parameters for Powder Mixed Electrical Discharge Machining of Inconel X-750 Alloy Using Taguchi-Topsis Approach.** *Journal Of Mechanical Engineering* 2021; **71**(1): 1 - 18.
- [4] Jadam T, Sahu SK, Datta S, Masanta M. **Powder-Mixed Electro-Discharge Machining Performance of Inconel 718: Effect of Concentration of Multi-Walled Carbon Nanotube Added to the Dielectric Media.** *Sādhanā* 2020; **45**(135):0123456789.
- [5] Karunakaran K, Chandrasekaran M. **Experimental Investigation Nano Particles Influence in NP MEDM to Machine Inconel 800 with Electrolyte Copper Electrode.** *Frontiers in Automobile and Mechanical Engineering* 7–9 July 2016; Sathyabama University, Chennai, India; p. 1-15.

- [6] Patel S, Thesiya D, Rajurkar A. **Effect Of Aluminium Powder Concentration On Powder Mixed Electric Discharge Machining (PMEDM) Of Inconel-718.** *Journal of Machining and Forming Technologies* 2017; **8**(1/2): 29-40.
- [7] Kumar A, Mandal A, Dixit AR, Das AK. **Performance Evaluation of Al₂O₃ Nano Powder Mixed Dielectric for Electric Discharge Machining of Inconel 825.** *Materials and Manufacturing Processes* 2018; **33**(9): 986-995.
- [8] Paswan K, Pramanik A, Chattopadhyaya S. **Machining performance of Inconel 718 Using Graphene Nanofluid in EDM.** *Materials and Manufacturing Processes* 2020; **35**(1): 33-42.
- [9] Bains PS, Singh S, Payal SHS, Kaur S. **Magnetic Field Influence on Surface Modifications in Powder Mixed.** *Silicon* 2019; **11**(1): 415-423.
- [10] Baseri H, Sadeghian S. **Effects of Nanopowder TiO₂-Mixed Dielectric and Rotary Tool on EDM.** *The International Journal of Advanced Manufacturing Technology* 2016; **83**: 519-528.
- [11] Ranjan A, Chakraborty S, Kumar D, Bose D. **An Investigation on Surfactant Added PMWEDM of Inconel 718.** *International Journal of Automotive and Mechanical Engineering* 2020; **17**(3): 8140-8149.
- [12] Reddy VV, Madar AKP. **Influence of Surfactant and Graphite Powder Concentration on Electrical Discharge Machining of PH17-4 Stainless Steel.** *The Brazilian Society of Mechanical Sciences and Engineering* 2015; **37**(2): 641-655.
- [13] Kolli M, Kumar A. **Effect of Dielectric Fluid with Surfactant and Graphite Powder on Electrical Discharge Machining of Titanium Alloy Using Taguchi Method.** *Engineering Science and Technology, an International Journal* 2015; **18**(4): 524-535.
- [14] Talla G, Gangopadhyay S, Biswas CK. **Influence of Graphite Powder Mixed EDM on the Surface Integrity Characteristics of Inconel 625.** *Particulate Science and Technology* 2017; **35**(2): 219-226.
- [15] Jabbaripour B, Hossein M, Reza M, Faraji H. **Investigating Surface Roughness, Material Removal rate and Corrosion Resistance in PMEDM of TiAl Intermetallic.** *Journal of Manufacturing Processes* 2013; **15**(1): 56-68.
- [16] Jafarian F. **Electro Discharge Machining of Inconel 718 Alloy and Process Optimization.** *Materials and Manufacturing Processes* 2020; **35**(1): 95-103.
- [17] Ming W, Xie Z, Cao C, Liu M, Zhang F, Yang Y, et al. **Research on EDM Performance of Renewable Dielectrics under Different Electrodes for Machining SKD11.** *Crystals* 2022; **12**(2): 291, (1-21).
- [18] Ming W, Xie Z, Cao C, Liu M, Zhang F, Yang Y, Guo X. **Optimization of Process Parameters and Performance for Machining Inconel 718 in Renewable Dielectrics.** *Alexandria Engineering Journal* 2023; **79**(7): 164-179.